

A Pulsed Muon Synchrotron for a Neutrino Factory

Version 1 10/12/02

Scott Berg, Al Garren, Bob Palmer,
G. Rees, Don Summers, Y. Zhao

Abstract

Following Don Summers ideas presentation at Nufac02, the paper considers a 4 to 16 GeV pulsed muon synchrotron accelerator for a Muon Collider. The paper discusses: 1) possible acceptance requirements, 2) arc and straight section lattices, 3) optimization of the magnet gradient for minimum stored magnetic energy, 4) the use of a DC offset for the pulsed ring magnets, 5) a preliminary look at the cost of a specific design, and 6) a parametric study of both pulsed synchrotron and RLA costs as a function of acceptances and allowed decay loss.

We conclude that if a decay loss of 25 % is acceptable, then a pulsed synchrotron with acceptances required using either one or two cooling rings, should reduce the 4-20 GeV acceleration cost by a factor of two compared with study-2.

Contents

1	Introduction	3
1.1	Neutrino Factory Feasibility Studies	3
1.2	Cost Reduction	3
1.3	Required Acceptances of Accelerator	4
1.4	Don Summers' pulsed synchrotron concept	4
2	Requirements	5
3	Lattice	5
3.1	Arc Lattice	5
3.2	Super Periods	6
3.3	Momentum vs. Bend Field Tracking Errors	7
3.4	Straight Lattice	8

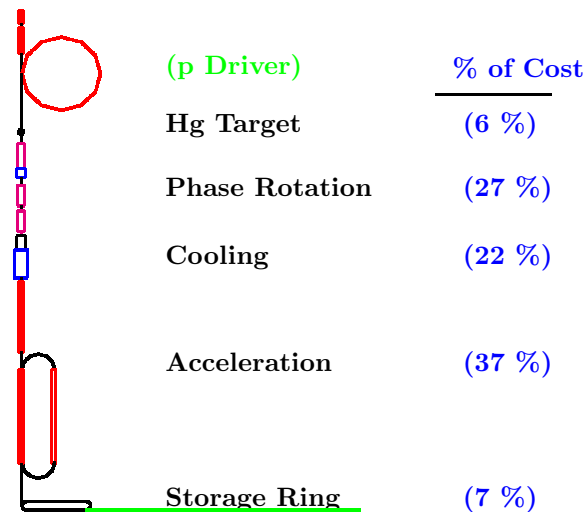
4	Super Conducting RF	8
4.1	Injection/Extraction	9
4.2	The full lattice	10
5	Pulsed Magnet Optimization	10
5.1	Introduction	10
5.2	Required Ave. Gradient vs. Decay Loss	10
5.3	Required Momentum Acceptance	11
5.4	Magnet Field Gradient Dependencies	11
5.5	Magnet Gradient Optimization	13
6	Magnet Design	14
6.1	General	14
6.2	Magnet Losses	15
6.2.1	DC cable heating	16
6.2.2	Eddy Currents Losses in Cables	16
6.2.3	Eddy Currents in Laminations	17
6.2.4	Eddy Currents in End Laminations	18
6.2.5	Hysteresis	19
6.2.6	Loss Summary	19
7	Pulsed Power Supply	19
7.1	Requirements	19
7.2	Pulsing Circuit	20
8	Baseline Costs	22
8.1	SC Linac	22
8.2	Pulsed Magnets	22
8.3	Pulsed Power Supplies	22
8.4	Vaccum and Diagnostics	23
8.5	Kickers	23
8.6	Civil	24
8.7	summary	24
8.8	total	24
9	Parametric Studies	24
9.1	Pulsed Synchrotron Costing Formula	25
9.2	Cost vs. Allowed Decay Loss	25
9.3	Cost vs. Acceptance	26
9.4	Comparison of Pulsed Synchrotron vs. RLA Costs	26
9.5	Summary of Pulsed vs. RLA comparisons	29
10	Conclusion	29

1 Introduction

1.1 Neutrino Factory Feasibility Studies

The second US Feasibility Study of a muon based neutrino source had simulated performance approximately six times better than the first study, and, if driven from a 4 MW proton source, appeared to meet the physics goals that had been set early in our considerations. But the estimated price (with 10% for missing items, but no contingency or overhead, and without the driver) was estimated to be approximately 1.74 B\$.

Although it is hard to quantify, it has widely been suggested that this cost is too high for the physics potential, good though that is. It is clearly very desirable to lower the cost, and a target of lowering it by a factor of two seems appropriate.



1.2 Cost Reduction

The main components of a neutrino factory are indicated in the above figure, together with the fractions of the total (driver excluded, and site utilities distributed) contributed by each. Suggestions have already been discussed¹ that would substantially reduce the cost of phase rotation. A cooling ring² should substantially cut the cooling cost. The RFOFO ring has components very similar to those in study-2, but uses only 33 m of them. compared with 108 m in study 2.

But cutting the cost of these two components, even by somewhat more than a factor of two, will not reduce the total sufficiently. We need to reduce the acceleration cost: the largest single percentage, by a similar factor.

¹Neuffer bunched beam phase rotation

²e.g. RFOFO Cooling Ring

This may become possible for two reasons:

1. The use of one or two cooling rings could significantly reduce the emittance of the muons, making it easier and cheaper to accelerate them. We will consider the use of both one, and two rings in this paper.
2. Alternatives to the RLA's (used in studies 1 and 2) may well be cheaper: both FFAG's and a pulsed synchrotron have been suggested. It is this second idea that is discussed here.

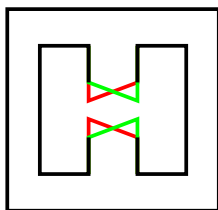
1.3 Required Acceptances of Accelerator

The following table gives the specified acceptances. transverse and longitudinal, for study-2 and plausible specifications for cases where either one or two cooling rings are employed. The numbers given for one ring are reasonably well justified by results of simulations. Those for two rings are more speculative.

	Study-2	1 ring	2 rings
Trans Acceptance (π mm rad)	15	15	4
Long Acceptance (π mm rad)	150	35	35

1.4 Don Summers' pulsed synchrotron concept

Don has proposed to replace the RLA, or RLA's in neutrino factories or Muon Colliders, with rapidly pulsed synchrotrons. Multiple arcs are no longer needed, allowing more turns and less acceleration per turn. The challenge in this approach is to design and build accelerator magnets that can be pulsed at rates corresponding to many kHz: far higher than more conventional fast cycling machines such as the Fermilab Booster (15 Hz), or RAL ISIS (50 Hz), but involving frequencies no higher than those commonly handled in laminated iron cored audio transformers.



Specifically, Don proposed the use of alternating gradient combined function magnets to minimize the eddy currents associated with non-planar fields passing through laminations at magnet ends. These magnets can be very long, with the field gradient alternating many times. This approach has the added advantage that it avoids a cost penalty associated with the number of elements. It allows the focus strength to be increased to minimize the pulsed energy, even as this decreases the cell lengths and increases their number.

2 Requirements

Consider, for instance,

1. Linac: .2 to 1 GeV/c
2. RLA: 1 to 4 GeV/c
3. Pulsed Synchrotron: 4 to 20 GeV/c

Assuming it is filled from a cooling ring similar to the RFOFO ring that has been discussed, then the specifications would be as given in the following table:

Initial Energy	E_{in}	(GeV)	4.0
Final Energy	E_{out}	(GeV)	20.0
Assumed Proton Power	P_p	MW	4
Muons/proton	$N_{\mu/p}$		0.15
Muons/bunch train	N_{μ}		$5 \cdot 10^{12}$
Bunch and RF Frequency	f_{RF}	(MHz)	201
Bunches/train	n_{bunches}		10
Length of train	ℓ_{train}	(m)	15
Effective Repetition Rate	f_{rep}	(Hz)	30
Acceptable decay loss	ξ	(%)	15-25
Normalized Trans. Acceptance	A_{\perp}	(π mm radians)	4
Normalized Longitudinal Acceptance	A_{\parallel}	(π mm radians)	35

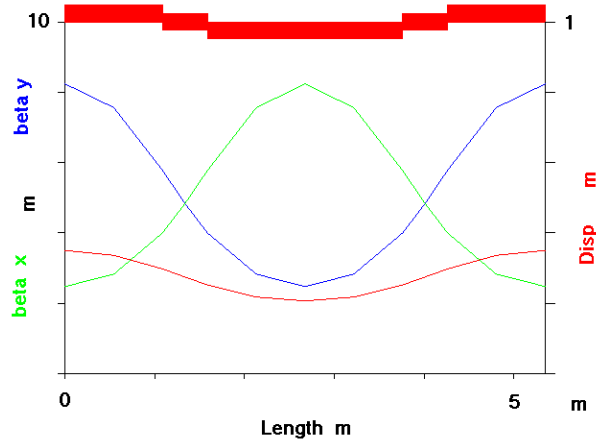
3 Lattice

3.1 Arc Lattice

As discussed in section 1.4, it is proposed that the arcs are formed by sequences of combined function cells formed within continuous long magnets, whose poles are alternately shaped to give focusing gradients of each sign. This design, in its strict implementation, implies very long magnets that would be difficult to transport, implies relatively high pulse voltages, and would make the insertion of trim coils difficult. However, the discussion in section 6.2.4 suggests that, if copper plate ends are used, then the magnet could be subdivided. We will however continue with the design assuming that they are continuous: breaking them up will only make things easier.

An example of such a cell has been simulated using SYNCH³. The example has gradients that alternate from positive 20 T/m gradient (2.24 m long), to zero gradient (.4 m long) to negative 20 T/m gradient (2.24 m) to zero gradient (0.4 m), etc. The relatively short zero gradient section is included to approximate a smooth change in the gradients. The Bending field of 0.9 T is uniform along the magnet. Lattice parameters vs, length for one cell of this lattice are plotted below.

³Courant et al

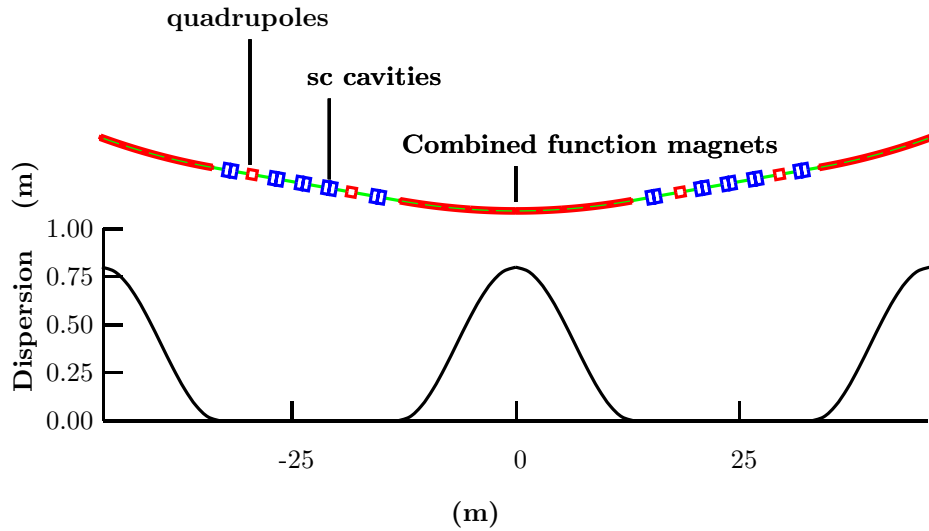


Parameters are:

Cell length	m	5.28
Combined Dipole length	m	2.24
Combined Dipole B_{central}	T	0.9
Combined Dipole Gradient	T/m	20.2
Pure Dipole Length	m	0.4
Pure Dipole B	T	1.8
Momentum	GeV/c	20
Phase advance/cell	deg	72
beta max	m	8.1
Dispersion max	m	0.392
Bend/cell	rad	0.0785*

3.2 Super Periods

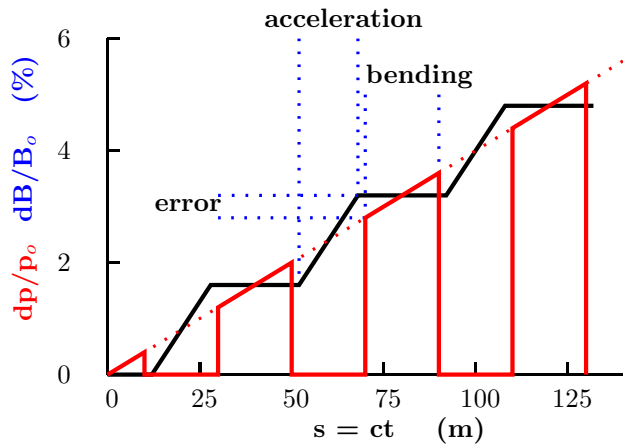
It is proposed to use 5 such arc cells (possibly all in one magnet) to form an arc segment. These segments being alternated with straight sections containing RF. The phase advance through one arc segment is $5 \times 72 = 360$ degrees. This being so, dispersion suppression between straights and arcs can be omitted. With no dispersion in the straight sections, the dispersion performs one full oscillation in each arc segment, returning to zero for the next straight. See the following figure. The extra aperture for the resulting doubling of the maximum dispersion will be included in the calculations of required aperture.



There will be 18 such arc segments and 18 straight sections, forming the 18 super periods in the ring.

3.3 Momentum vs. Bend Field Tracking Errors

The RF must be distributed around the ring with sufficient frequency to avoid large differences between the beam momentum (which increases in steps at each RF section) and the arc magnetic field (which is increasing continuously). See the following figure.



If the field is controlled such that the field matches the momentum at the center of each arc section, and each arc section has a uniform transfer function (Field/Current), then the maximum absolute momentum error Δp is

$$\Delta p_{\text{Max}} = \frac{1}{2 n_{\text{turns}} m_{\text{RF Stations}}} (p_2 - p_1)$$

which, for 12 turns and 18 super periods, is $\times 16/(2 \cdot 12 \cdot 18) = .037 \text{ GeV}/c$. At injection this would correspond to 0.92 % which is significant, because at injection the beam is already large, so the beam pipe and magnet aperture would have to be enlarged to accept the additional momentum errors.

This problem can be removed if the magnets are so designed that, for the same current, the field is higher at the start of each arc segment, and less at the end. With the appropriate variation, the tracking can be made perfect at one momentum. If we do this for the injection momentum then no increase in aperture is required. At higher energy the correction progressively fails, till at ejection, the mismatch is 0.83 %. But this does not require any additional aperture, because the beam is smaller at higher energies, and there is adequate space in the pipe for the momentum errors.

If greater decay loss is acceptable, then acceleration occurs over more turns, less RF is needed, and it is reasonable to have fewer super periods, but it will be seen that the tracking mismatch remains the same.

3.4 Straight Lattice

Straight sections without dispersion are used to contain superconducting RF, and, in two longer straights, the injection and extraction. In order to assure sufficiently low magnetic fields at the cavities, and to efficiently use the space, relatively long field free regions are desirable. A straight consisting of two half cells of the following lattice would allow a central gap of 10 m between quadrupoles, and two smaller gaps at the ends.

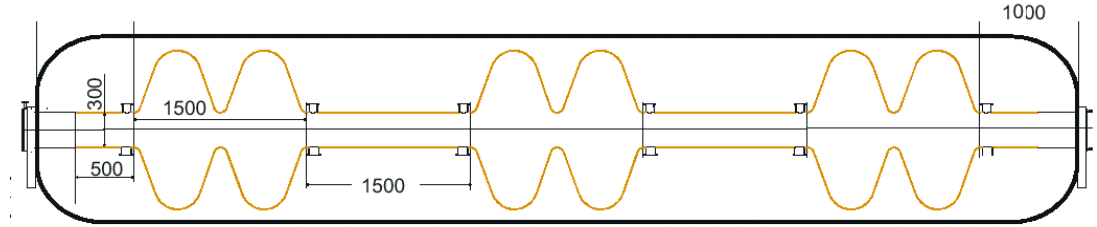
ϕ	deg	77
$L_{\text{cell}}/2$	m	11
L_{quad}	m	1
dB/dx	T/m	7.54
a	cm	5.8
β_{max}	m	36.6
σ_{max}	m	.0195
B_{pole}	T	0.44
$U_{\text{mag/quad}}$	J	≈ 3000

4 Super Conducting RF

The SC RF design taken is very similar to that in Study-2, with parameters as given in the following table:

Frequency	MHz	201
Gap	cm	75
Grad	MV/m	15
Stored Energy	kJ	1.1
Muons per train		$5 \cdot 10^{12}$
Passes		12

The RF and cryostat for the 10 m long space between quadrupoles is illustrated below.



The energy given to the beam ΔU_{beam} is:

$$\Delta U_{\text{beam}} = n_{\text{turns}} N_{\mu} q_{\mu} \mathcal{E} L_{\text{gap}}$$

which for 12 turns, $5 \cdot 10^{12}$ muons, 15 MV/m, and 75 cm, is 110 Joules. The stored energy is approximately 900 Joules, giving an energy loading of 8.2 %, and a voltage drop during acceleration of 4 %.

4.1 Injection/Extraction

Little consideration has been given to the kicker design and the injection and extraction channels. If we take the parameters such as to give a deflection 2 times the minimum needed to separate the phase space from that of the beam, then the required deflection is

$$\Delta p_y = 2 \times B_x L c = m_{\mu} 2 f_{\sigma} \sqrt{\frac{A_{\perp} \beta \gamma}{\beta_y}}$$

requiring a kicker field, voltage and stored energy:

$$B_x = 2 \times \frac{\Delta p_y}{L c} = \frac{m_{\mu} 2}{L c} \sqrt{\frac{A_{\perp} \beta \gamma}{\beta_y}}$$

$$V = 2 \times \frac{B_x Y L}{t_{\text{rise}}} = \frac{4 m_{\mu}}{c} \frac{A_{\perp}}{t_{\text{rise}}}$$

$$U = 4 \times \frac{B_x^2 L X Y}{2 \mu_o} = \frac{m_{\mu}^2 8}{\mu_o c^2} \frac{A_{\perp}^2}{L}$$

For $t=500$ nsec, $A_{\perp}=4 \pi$ mm, $L=4$ m, then $V = 2 \times 4.5 = 9$ kV, and $U = 4 \times 4.7 = 19$ J.

These parameters are similar to those in existing \bar{p} accumulator rings, and should not be difficult.

4.2 The full lattice

The total number of quadrupoles is $16 \times 2 + 2 \times 4 = 40$. The total quadrupole stored magnetic energy is 117 kJ, or about 7 % of the total with the arcs. The full circumference is $18 \times 26.5 + 16 \times 22 + 2 \times 44 = 917$ m.

Matching between the arcs and straights is not yet designed

5 Pulsed Magnet Optimization

5.1 Introduction

The previous section has described a lattice with specific bending fields and gradients. These values were obtained from a cost optimization, based on reasonable assumptions for pulsed magnet, power supply, and RF costs. The procedure followed will now be discussed.

5.2 Required Ave. Gradient vs. Decay Loss

The required average acceleration gradient around the ring $\mathcal{E}_{\text{ring}}$ is given by:

$$\mathcal{E}_{\text{ring}} = \frac{m_{\mu}}{\tau_{\mu}} \frac{\ln\left(\frac{E_2}{E_1}\right)}{\ln(1 - \xi)}$$

where τ_{μ} is the muon lifetime, and E1 and E2 are the initial and final energies. With values taken from the above table, and decay loss $\xi=15\%$, then $\mathcal{E}_{\text{ring}} = 1.58$ MV/m.

If the RF is confined to dispersion free straight sections, where the fraction of length taken up by RF gaps is χ , the RF gradient in the gaps is \mathcal{E}_{gap} , the voltage drop from loading is ϵ , and the phase is ϕ , then the average gradient in those straights is:

$$\mathcal{E}_{\text{straights}} = \mathcal{E}_{\text{gap}} \chi (1 - \epsilon) \cos(\phi)$$

For $E=17$ MV/m, $\chi=22\%$, $\epsilon=5\%$, and $\phi=20$ deg, then $\mathcal{E}_{\text{straights}} = 3.3$ MV/m
The required ratio of straights to arcs is then:

$$\frac{\text{Straight}}{\text{Arc}} = \frac{1}{\left(\frac{\mathcal{E}_{\text{straight}}}{\mathcal{E}_{\text{ring}}} - 1\right)}$$

which gives, with the above parameters, Straight/Arc ≈ 0.9 ; i.e. almost equal lengths for the straights and arcs. **If instead we allow 25% loss, then Straight/Arc ≈ 0.4 : a significant saving.**

5.3 Required Momentum Acceptance

The required momentum acceptance Δ_p is given by:

$$\Delta_p = \sqrt{\frac{A_{\parallel}}{\beta_{\parallel} (\beta_v \gamma)}}$$

where

$$\beta_{\parallel} = \frac{1}{2\pi} \sqrt{\frac{\gamma \lambda_{RF} m_{\mu} \eta}{\mathcal{E}_{\text{Ring}} \sin(\phi)}}$$

and

$$\eta \approx \frac{D_{\text{ave}}}{R}$$

For the ring we will describe, $\Delta p \approx 1\%$.

5.4 Magnet Field Gradient Dependencies

We wish to minimize the total pulsed energy needed. We will therefore examine this energy as a function of the magnitude of the gradients used.

The maximum magnetic field will be limited by saturation at the high field side of the gradient. This gives a relationship between the median bending field and the magnitude of the gradient. A larger gradient will imply a lower bending field, a larger ring circumference, more RF, and more arc magnets. But a weaker gradient will give less focusing, the need for larger apertures, and thus magnets with more stored energy per unit length.

Scaling from the Synch lattice discussed above (section 3.1):

$$\beta_{\perp}(\text{max}) = 8 \text{ (m)} \frac{20 \text{ (T/m)}}{G_B}$$

$$D_{\text{max}} = 2 \times 0.4 \text{ (m)} \frac{\beta_{\perp}(\text{max})}{8 \text{ (m)}}$$

The factor of 2 in this expression is introduced to allow for uncorrected Dispersion swings discussed in section 3.2. The vertical and horizontal half apertures are given by

$$a_y = \sqrt{\frac{\beta_{\perp} A_n}{\beta \gamma}}$$

$$a_x = \sqrt{a_y^2 + (D \Delta_p)^2}$$

Assuming that, for field quality, the gradient must be extended 50% beyond the horizontal half aperture, then for a given maximum allowed field B_{max} , the central bending field B_o is related to the magnetic field Gradient of G_B

$$B_o = B_{\max} - 1.5 a_y G_B$$

B_{\max} was taken to be 2.0 T, which should be within the saturation limit of Silicon steel (see section 6.1).

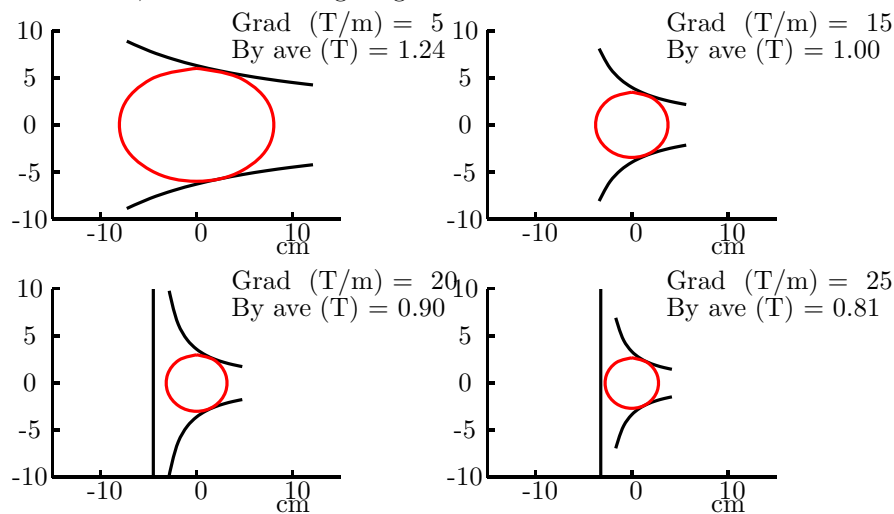
We require a field linear in x: $B_y = B_o + G x$. To obtain this we need a vertical gap g_y :

$$g_y = 2 A_y \left(1 - \frac{B_o}{G x}\right) \left(1 + \frac{G(\text{T/m})}{100}\right)$$

The second factor in parentheses is needed to avoid the sloping pole faces from interfering with the elliptical beam pipe.

When the field at one side of the magnet approaches zero, the gap goes to infinity. In this case, an iron 'mirror' plate is introduced at the position for zero gradient. The magnet is then equivalent to one half of a quadrupole with the mirror plane down the middle. Such magnets have been used before, as in the SLC arcs.

The following figure gives examples of cross sections of magnets that meet these criteria, for different magnet gradients:



The Required integrated arc length is $2\pi P_2/(c B_o)$ and the stored magnetic energy per unit length is approximately:

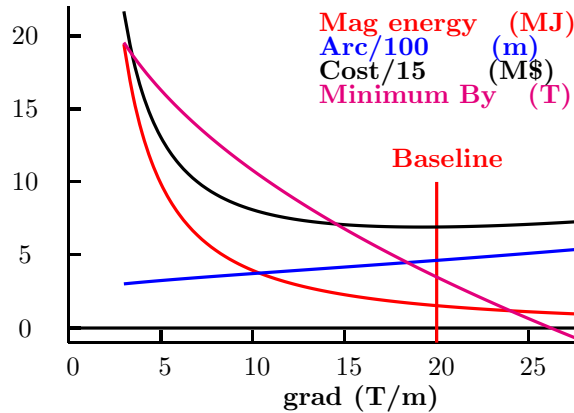
$$\frac{U}{L} \approx 2 \times \frac{1}{2 \mu_o} A_y A_x B_o^2 \left(1 + \frac{G(\text{T/m})}{100}\right)$$

The factor of 2 approximates the additional filed energy outside the 'good' field region. Note that the gradient does not enter this expression since, despite the energy dependence on B^2 , the differential stored energy $\propto g(x) B^2$ is linear in x, and its average is equal to that at the center.

5.5 Magnet Gradient Optimization

Below, we plot the arc magnetic stored energy, the total arc length, the minimum B_y in the combined function magnets, against the magnet gradients. The costs given are calculated using estimates given in Section ??.

We Select the 20 T/m for the baseline design, which minimizes the total cost.



Parameters for selected field gradients are given in the following table: Note that the parameters in the table are only approximate, and do not exactly agree with those derived below. It is intended only to show how these parameters vary with the gradient chosen.

G T/m	2 a_x cm	2 a_y cm	B T	B1 T	B2 T	n	U MJ	V MV/m	arc m	str m	circ M\$	\$mag M\$	\$RF M\$	\$tot
5.0	11.59	18.95	1.29	0.82	1.76	17	9.91	0.96	325	285	610	145	52	196
9.0	8.64	12.56	1.15	0.59	1.72	15	4.54	1.08	364	319	682	70	58	128
13.0	7.19	9.76	1.05	0.41	1.68	14	2.77	1.19	400	350	750	46	64	110
17.0	6.29	8.14	0.96	0.27	1.65	12	1.92	1.29	435	382	817	35	69	104
21.0	5.66	7.07	0.89	0.14	1.63	11	1.43	1.40	472	414	886	29	75	104
25.0	5.18	6.30	0.82	0.03	1.61	11	1.11	1.52	511	448	960	25	81	106

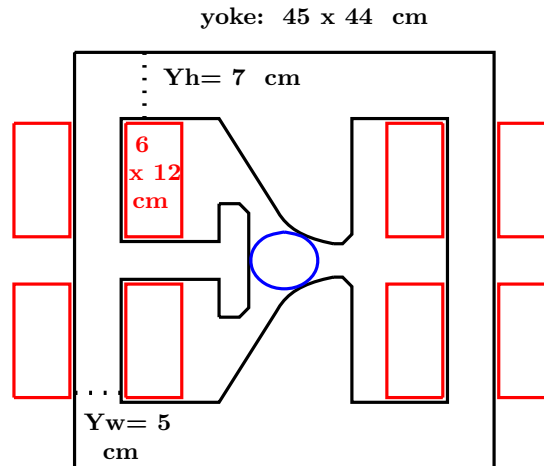
It is seen that the cost is minimized by a gradient that is close to the maximum set by the requirement that the field does not reverse sign and thus require a geometry different from that proposed. The optimized ring has very strong focusing, very short cells, and a resulting high tune (≈ 25). Accelerators, both fast and slow cycling are not usually built with such strong focusing. The lack of a penalty for the increased number of magnets may be one explanation. Another may be that problems related to chromaticity correction with such strong focusing may argue against such parameter choices. This later consideration may not apply here, when the acceleration takes place in so few turns. The ring should behave much like a transport line, and chromaticity correction should not

be needed.

6 Magnet Design

6.1 General

A sketch of the magnet cross section is shown below. There are two poles on the right side, with shapes essentially identical to those in one half of a quadrupole. On the left, there is a "mirror" plane attached to the return yoke. To minimize the voltage, there are two loops of conductors, each a single turn, around the flux returns (see section 7.1), although, if the magnet is broken into shorter parts to reduce maximum voltages (see section 6.2.4), then single loops might be preferred. This option would reduce both DC and pulsed energy losses.



Possible materials for the yoke⁴ are given in the following table.

Material	Composition	ρ Ω cm	B_{\max} T	H_c Oersteds	Thicknesses μm
Grain Oriented	3Si,97Fe	47	2.0	0.1	50,100,175
NKK Super E-Core	6Si,94Fe	82	1.8		50,100
Metglas 2605SA1	2C,3Si,14B, 81Fe	135	1.6	.03	30

Punching precision of the order of 25 μm should be sufficient.

We choose 100 μm grain oriented silicon steel because it has the highest saturation and, unlike metglas, can be easily stamped. The grain orientation in

⁴Summers, <http://arXiv.org/pdf/physics/0109002>, and H Sasaki, KEK-91-261

the poles would clearly be vertical, to use the most favourable properties at the highest field point of the poles.

It is not clear whether, if a single punched lamination is used, if it matters that the grain orientation is wrong along the top and bottom of the picture frame. A simple reduction in the magnetic μ , from 4000 to 1000 for instance, would have a negligible effect on the $\int B/(\mu\mu_o) d\ell$ compared to the gap, and would thus not effect the performance. If the saturation B in the wrong direction is somewhat less, then this merely requires that the height of the top frame Y_h be a little thicker than the sides Y_w . Only if the saturation field is much lower in the wrong direction do we need to make the yoke out of multiple pieces to keep the grain orientation in the favoured direction⁵.

The return yokes have been sized here to have approximately 1.4 T in the verticals and 1.0 T in the horizontals. The peak pole field, as specified above, is 2.0 T, but this occurs at a horizontal position 1.5 times the maximum 'good' aperture. Saturation effects might need to be corrected by appropriate hole punching in the laminations.

The single turn coils would consist of a large number of 0.5 mm (or possibly up to 1 mm) diameter individually insulated strands, formed into a cable, twisted, and epoxied into the required cross section with water cooling pipes embedded.

An alternative that should be looked at would be to form the conductors out of a stack of edge cooled insulated 0.5 mm thick copper sheets. In this case if there is no twisting, each sheet would terminate at a slightly different voltage, and would have to be connected to a separate pulsing circuit. Since a great multiplicity of individual SCR's will anyway be required, this may not be a serious difficulty. But if the windings were not on the returns, but conventionally on either side of the gap, then a geometry is possible with transposition from the outside going down the magnet, to the inside coming back. This might allow the ends to be joined.

6.2 Magnet Losses

The proposed pulse circuit will be discussed in section 7.2. It provides a nearly linear field ramp by adding a full cycle of pulsed current, a fourth harmonic pulsed current, and a DC component. The frequency of the pulse is approximately twice that of a simple half sin wave pulse, but because the AC component is reduced by a factor of two, the eddy current losses are the similar.

The single turn current at the maximum momentum of 20 GeV/c is 51.6 kA. The DC component is 0.6 times this value. The pulse frequency is 10.25 kHz, and its magnitude is 0.45 times the current at 20 GeV. With these values, we can calculate magnet losses.

⁵Summers Nufac-02

6.2.1 DC cable heating

For conductors as shown in the figure, and 70% packing, the cross section for both conductors is $2 \times 12 \text{ cm} \times 6.7 \text{ cm} \times 0.7 = 5.6 \cdot 10^{-3} \text{ m}^2$, with a resistance for length $2 \times 26.5 \text{ m}$, of

$$R = \frac{2 \times 26.5 \times 1.7 \times 10^{-8}}{5.6 \cdot 10^{-3}} = 0.161 \text{ m}\Omega$$

The power disipated by the "DC" current of $0.6 \times 51.6 \text{ kA}$, in the two return windings is then

$$P = 2 \frac{I^2 R}{2} = .3 \text{ MW per magnet}$$

or 4.4 kW/m of conductor, and 4.8 MW total.

4.8 MW dc loss is not serious, but it could be reduced substantially by slow pulsing of the "DC" component. For instance, if the DC component is reduced, but supplemented by a 30 Hz component, then the average loss can be reduced by a factor of 3, to 1.6 MW. It would also be halved if a conventional winding is used instead of windings about the flux returns.

6.2.2 Eddy Currents Losses in Cables

The skin depth δ :

$$\delta = \sqrt{\frac{2 \rho}{2\pi f \mu_o}}$$

which for copper ($\rho = 1.7 \cdot 10^{-8}$), and $f = 10.25 \text{ kHz}$, $\delta = 0.64 \text{ mm}$. Litz wire is available with diameters down to 0.25 mm, but 0.5 mm would seem adequate.

For a 0.1 T fringe field, the power disipated is approximately

$$\begin{aligned} P_{\text{Cu eddy}} &= \text{Vol} \frac{(2\pi f_{\text{pulse}} \Delta B_f w)^2}{24 \rho} \frac{f_{\text{rep}}}{f_{\text{pulse}}} \\ &= \text{Vol} \frac{(2\pi \Delta B_f w)^2}{24 \rho} f_{\text{rep}} f_{\text{pulse}} \end{aligned}$$

If w is taken to be the wire diameter of 0.5 mm, and the pulsed part of the stray field is $B_f = 0.45 \cdot 0.1 \text{ T}$, f_{rep} is 30 Hz, and f_{pulse} is 10.25 kHz, then

$$P_{\text{Cu eddy}} = 8 \times 26.5 \times .067 \times .12 \times 0.7 \times \frac{(2\pi \cdot 0.045 \cdot .0005)^2}{24 \cdot 1.7 \cdot 10^{-8}} \cdot 30 \times 10250 = 16.8 \text{ kW/magnet}$$

or, for 18 magnets: 303 kW, which is small compared with the DC loss. From the total power loss point of view, 1 mm wires, giving 1.2 MW loss, would be acceptable. However, these losses will lower the Q of the pulsing circuit, requiring more power to top-up the storage capacitors, and thus increasing the

power supply cost. More study would be needed to determine the cost optimum. This heating would also be halved if a conventional winding is used instead of windings about the flux returns.

In either case, cooling could be provided by water in stainless steel pipes epoxied into the multiwire cables, or possibly the wires could be replaced by edge cooled thin copper laminations (see section 6.1).

6.2.3 Eddy Currents in Laminations

The skin depth in iron, with a resistivity of $47 \cdot 10^{-8}$ and μ of 4000, at 10.25 kHz is

$$\delta_{\text{Fe}} = \sqrt{\frac{2\rho}{f_{\text{pulse}} \mu \mu_o}} = 53 \quad \mu\text{m}$$

For 100 micron laminations, the heating will be

$$\begin{aligned} P_{\text{Cu eddy}} &= \text{Vol} \frac{(2\pi f_{\text{pulse}} \Delta B_f w)^2}{24 \rho} \frac{f_{\text{rep}}}{f_{\text{pulse}}} \\ &= \text{Vol} \frac{(2\pi \Delta B_f w)^2}{24 \rho} f_{\text{rep}} f_{\text{pulse}} \end{aligned}$$

If w is .1 mm, and the pulsed part of the field is $B_f = 0.45$ T, f_{rep} is 30 Hz, and f_{pulse} is 10.25 kHz, then

$$P_{\text{Fe eddy}} = 26.5 \times 0.18 \frac{(2\pi \cdot 0.45 \cdot .0001)^2}{24 \cdot 47 \cdot 10^{-8}} 10250 \times 30 = 10 \text{ kW/magnet}$$

or 180 kW total, which is not significant, compared with the DC losses. From this criterion, 200 μm laminations, giving 720 kW total, would be acceptable. However, these losses will lower the Q of the pulsing circuit, requiring more power to top-up the storage capacitors, and thus increasing the power supply cost. Optimization is needed.

Another effect that must be considered is the loss of inductance due to the sum of eddy currents coupled to the driving current. For a closed iron inductor, this loss of inductance is given⁶ by:

$$\frac{\Delta L}{L} = \frac{1}{R} \frac{\sinh(R) + \sin(R)}{\cosh(R) + \cos(R)}$$

where

$$R = \frac{w}{\delta_{\text{skin}}}$$

Examples of the effect are given in the following table, and appear large unless very thin laminations are used.

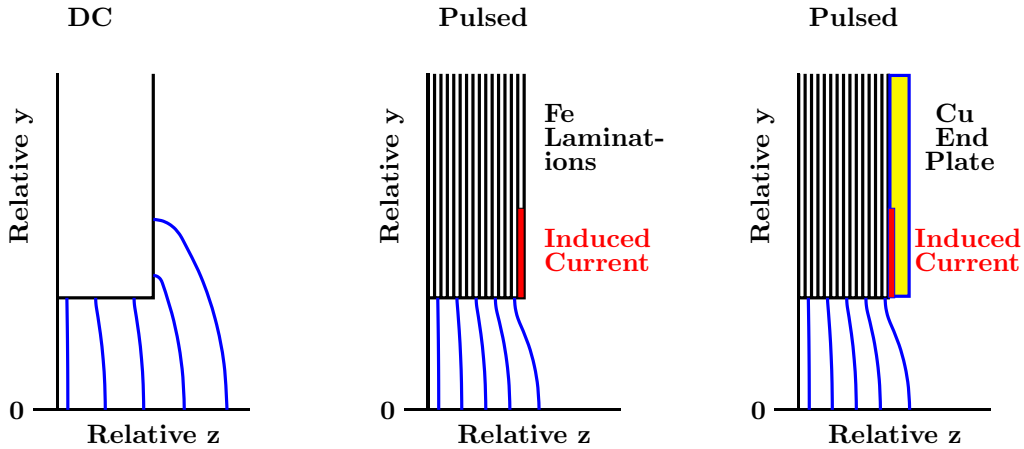
⁶Lorrain and Corson, 3rd edition, p537-542; and K L Scott, Proc. Inst. of Radio Engineers, 18 (1930) p1750-1764

Decay loss frequency	15	25
w	$\Delta L/L$	$\Delta L/L$
100 μm	27.8 %	12.8 %
75 μm	11.5 %	4.5 %
50 μm	2.6 %	0.9 %

In our case the inductance is dominated by the gap, and this effect on the inductance should be negligible. But it can give an indication as to the relative shielding of the iron by the eddy currents. This would only be important, however, near saturation, and near saturation the μ is low, the skin depth is large, and this relative screening goes away.

6.2.4 Eddy Currents in End Laminations

In a steady state, at the end of a magnet, the field lines leave the end horizontally up to a vertical distance of the same order as half the magnet gap (see following figure). These lines of force are passing through the end lamination. If pulsed, eddy currents will be induced in the end lamination such as to restrain such field lines to within a skin depth of the edge.



What follows is an order of magnitude calculation only. The induced current density in this edge is, very approximately:

$$i_{\text{edge}} \approx \frac{dI_{\text{edge}}}{dy} \approx \frac{B_{\text{pulse}}}{2 \mu_o}$$

and will extend upwards for a distance of the order of the half gap $g/2$. The heating W per end is then:

$$W \approx \frac{i_{\text{edge}}^2 X \rho_{Fe}}{\delta_{\text{skin}}} a_y \frac{f_{\text{rep}}}{2 f_{\text{pulse}}}$$

where $X \approx 4 a_x$ is the pole width. For $B_{\text{pulse}} = 0.45 \text{ T}$, $\rho_{Fe} = 47 \cdot 10^{-8}$

$$W \approx \left(\frac{0.45 \text{ T}}{2 (4\pi \cdot 10^{-7})} \right)^2 \frac{0.2 \cdot 47 \cdot 10^{-8}}{53 \cdot 10^{-6}} \cdot 0.03 \frac{30}{2 \cdot 10250} \approx 10^4$$

10 kW per end: or 360 kW for the long magnets, assuming that the gradient reversals are slow enough to avoid this effect, and assuming the quadrupoles are made of ferrite. With separate magnets for each gradient, the total would have been of the order of $18 \times 10 \times 10 \text{ kW} = 1.8 \text{ MW}$: a very significant effect, and one that lead to the continuous magnet concept used in this proposal.

However, if a copper plate is inserted at the end of each magnet, then the heating drops to:

$$W \approx \left(\frac{0.45 \text{ T}}{2 (4\pi \cdot 10^{-7})} \right)^2 \frac{0.2 \cdot 1.7 \cdot 10^{-8}}{0.64 \cdot 10^{-3}} \cdot 0.03 \frac{30}{2 \cdot 10250} \approx 30$$

which is not a problem. This is important because, if true, it would allow the arc magnet to be broken into smaller parts, lowering the voltages, and allowing tuning.

6.2.5 Hysteresis

Hysteresis losses are proportional to the number of cycles, which are less than in ISIS, and only a factor of 2 more than the Fermi Booster. They will not be a significant problem here.

6.2.6 Loss Summary

These results are summarized in the following table

DC Ohmic Heating (with 'pulsed' DC)	4.8 MW (1.6 MW)
Eddy Current Heating in .5 mm (1 mm) wires	300 kW (1.2 MW)
Eddy Current Heating in 100 μm (200 μm) laminations	180 kW (0.72 MW)
Eddy Current Heating at magnet ends with (without) Cu plates	$\approx 3 \text{ kW}$ ($\approx 360 \text{ kW}$)
Hysteresis Loss	small
DC total	4.8 (1.6) MW
Pulsed	0.48 (2.3) MW

7 Pulsed Power Supply

7.1 Requirements

The single turn current I is

$$I \approx \frac{B_o 2 a_y}{\mu_o} \left(\frac{1 + \text{Grad(T/m)}}{100} \right)$$

which for our case is 51.6 kA.

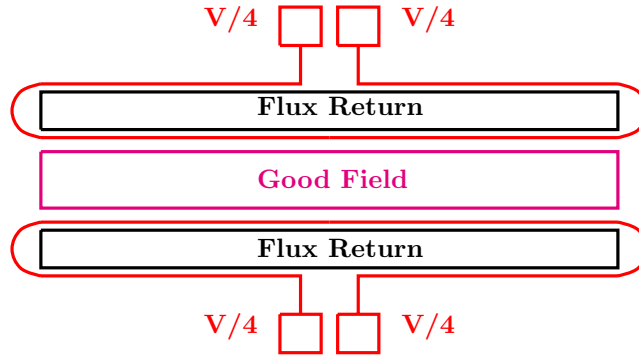
The ramp time t depends on the specified decay loss ζ :

$$t = \frac{\Delta E \tau_\mu}{m_\mu} \frac{\ln(1 - \zeta)}{\ln(E2/E1)}$$

which for $\zeta = 15\%$ is 35μ sec., and for $\zeta=25\%$ is 52μ sec. The single turn Voltage V is

$$V = \frac{d\Phi}{dt} = 2 \frac{2 a_x L B_o}{t}$$

For a continuous magnet through 5 cells, the length is 26.5 m. The total Voltage for a single loop around the poles is then 99 kV [for 25% loss, it is 60 kV]. This can be reduced either by breaking the magnet into shorter sections. It can also be reduced by applying loops around the flux returns, and by driving the loops in a push-pull arrangement:



The inductance per magnet ($2 \times$ the inductance of either loop) is

$$L = \frac{V}{I} t = 67.1 \mu \text{ H}$$

7.2 Pulsing Circuit

A simple pulse circuit consisting of a single capacitor, a switch and the magnet inductance would give a half sin wave pulse and acceleration that is very far from uniform, and require the switches to handle the full current and voltage.

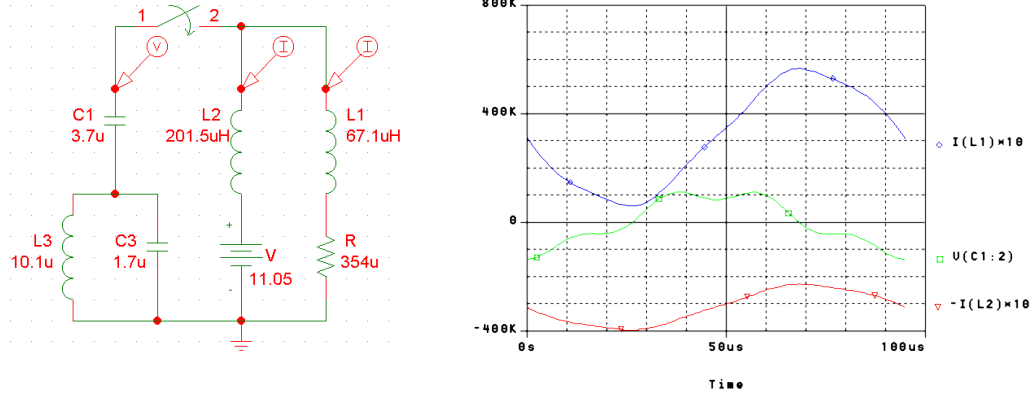
The volt-amps switched can be reduced, as in most fast cycling accelerators, by adding a DC component. This component is maintained by adding a second inductor (L2) in parallel with the magnet (L1), with the dc current set up in the loop of the two inductors. In this example, the DC current chosen is 45 %

of the current required at the ejection energy, thus reducing the needed pulse current to 55% and the switched power, under ideal conditions, to 22%.

The switch current is increased by a factor $(1+L1/L3)$ by the current shorted through the second inductor. And it is somewhat increased by the need to have the ejection current a little below the peak.

A harmonic circuit to flatten the voltage and thus straighten the current ramp has also been included.

The following figure at left show the proposed circuit with parameters for one 26.5 m magnet with a single conventional turn. On the right are PSPICE simulated traces of the voltage and current on the magnet, and the current in the choke loop.



The field rise is linear to within $\pm 1\%$ of the maximum. The following figure shows the variation in the rate of rise, which is only $\pm 10\%$ compared with the 100% variation in the $\pi/4$ case.

The maximum pulsed magnet current $I_{\text{pulse}} = 270 \text{ kA}$

The pulsed energy to the magnet is thus $L_{\text{mag}} I_{\text{pulsed}}^2 = L (270\text{k})^2$

The pulsed Energy including the choke is

$$U_{\text{with DC}} = 1.33 \times L_{\text{mag}} I_{\text{pulsed}}^2 = 1.33 L (270\text{k})^2$$

This can be compared with that needed if a simple half wave pulse were used: where $I_{\text{simple}} = 570 \text{ kA}$. and Pulsed Energy

$$U_{\text{simple}} = L_{\text{mag}} I_{\text{simple}}^2 = L (570\text{k})^2$$

so

$$\frac{U_{\text{with DC}}}{U_{\text{simple}}} = \frac{1.33 L (270)^2}{L (570)^2} = 0.3$$

The parameters are summarized:

$\Delta(\text{dB}/\text{dt})$	$\pm 10\% \dagger$
B_{DC}	$0.6 \times B_{20 \text{ GeV}}$
B_{max}	$1.05 \times B_{20 \text{ GeV}}$
$B_{switched}$	$0.49 \times B_{20 \text{ GeV}}$
f (kHz)	10.25
$U_{switched}/U_{half \text{ wave}}$	30 %

\dagger A further harmonic could be used to reduce this, if required.

8 Baseline Costs

8.1 SC Linac

Scaling from Study-2 which, for 4.38 GeV, had 63 M\$ for cavities and 89 M\$ for power supplies, and 10 M\$ for cryogenics. We double the cryogenic cost because of more complicated cryostats, giving:

$$63/4.38 = 14.4 \text{ M\$/GeV for Cavities}$$

$$89/4.38 = 20.3 \text{ M\$/GeV for RF power.}$$

$$28/4.38 \times 2 = 12.8 \text{ M\$/GeV for cryogenics}$$

For a total of 47.5 M\$/GeV, compared with 41.1 M\$/GeV in study 2; i.e. a fudge factor of 1.16. Multiplied by our required acceleration of $16(\text{GeV}) / 12(\text{turns}) = 1.33 \text{ MV}$, with a correction of 5% for loading, gives $1.33 \times 1.05 \times 47.5 = 66.5 \text{ M\$}$ for the SC RF.

8.2 Pulsed Magnets

The cost of the 15 Hz pulsed booster magnets at Fermilab are approximately 1.93 \$/J for dipoles, and 5.45 \$/J for quadrupoles⁷. If we use an average of 3.7 \$/J for our combined function magnets, and multiply both this by 2 to allow for the use of thinner laminations and Litz cable, then the cost is 7.4 \$/J for the combined function magnets and 10.9 \$/J for the quads. Multiplied by the 1.59 MJ and 0.12 MJ respectively, we obtain an estimate of $11.3 + 1.3 = 12.6 \text{ M\$}$ for the pulse magnets.

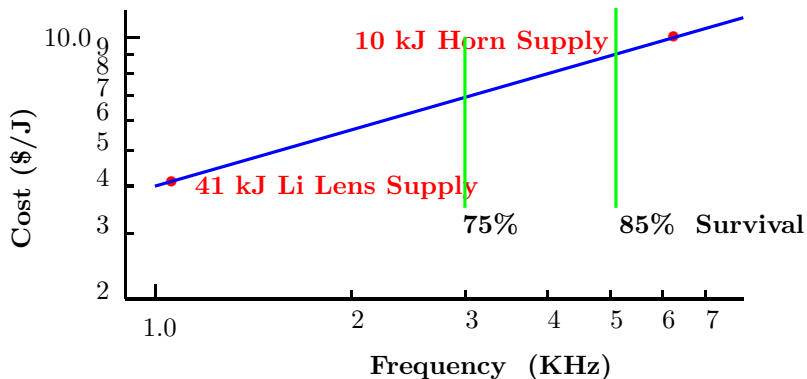
8.3 Pulsed Power Supplies

To estimate the cost of the pulsed power source we have looked at the cost of two FNAL pulsed supplies:

1. A 10kJ, 80 microsecond half sin wave (6.25 kHz) pulser, costing 30 k\$ parts + 40 k\$ labor in 1995 = 100 M\$ if inflated at 5% per year, or 10 \$/J.
2. A 41 kJ, 470 μ sec half wave (1.06 kHz) costing 120 k\$ in 1995 = 168 k\$ inflated, or 4 \$/J.

⁷Rees

These are plotted on a log log scale below.



These two are consistent with a cost of $4 \times \sqrt{f(kHz)}$ \$/J, which gives 12.8 \$/J for our 10.25 kHz frequency.

No increase has been included for the admittedly more complicated pulse circuit, but no reduction has been claimed for the quantity or size discount: our pulse energy is two orders of magnitude higher than these examples.

With no DC offset then the Pulse Supplies will cost: $(1.59 + 0.12) \times 12.8 = 21.9$ M\$

With the DC offset, as proposed, then the switched energy is reduced to 30% to 6.57 M\$, to which must be added the cost of chokes with 3 times the magnet energy ($1.71 \times 3 = 5.13$ MJ), which, at 1.5 \$/Joule (FNAL), adds $5.13 \times 1.5 = 6.7$ M\$, giving a total of $6.57 + 6.7 = 13.3$ M\$.

Optimizing the inductance of the chokes lowers this cost to 11.6 M\$, but this is not included in the baseline cost quoted below.

8.4 Vacuum and Diagnostics

Costs are scaled from the Study 2 RLA in proportion to the total vacuum lengths. The RLA costs were $15 + 4 = 19$ M\$ for (720m linacs + 7 x 363m arcs) 3261m, giving 5.8 k\$/m. When multiplied by our 917 m circumference gives 5.34 M\$.

8.5 Kickers

We have as yet no cost estimate for the kickers, but they will be of the same order as those in antiproton accumulators, and these are not dominant costs.

8.6 Civil

We scale again from study 2 cost of 19 M\$, in proportion to total tunnel length of (720 linacs + 2 x 363 arcs) 1446 m, giving 13.13 k\$/m. When multiplied by our 917 m circumference, we get 12.0 M\$.

8.7 summary

The costing is summarized in the following Table:

Item	Scaling	Fudge	Cost M\$
SC Acceleration	$\Delta E=1.39$ GV	1.16^1	66.5
Pulsed Magnets	Stored Energy=1.59 + 0.12 MJ	2^2	12.6
Pulsed Supplies	Switched Energy=0.51 MJ at 10 kHz	1	6.6
Chokes	Stored Energy=5.1 MJ	1	6.7
Vaccum and Diagnostics	Length of Beam pipe=917 m	1	5.3
Civil	Length of Tunnel=917 m	1	12
Kickers			?
Total			109.7
Study-2			385

Note 1) Correction for more shorter cryostats

Note 2) Correction for higher frequency

8.8 total

The total is $66.5+12.6+13.3+5.3+12=109.7$ M\$, plus the cost of the kickers. This might be compared with the Study 2 RLA without the transfer lines, but with civil construction, corrected for its greater total acceleration: $(436-34+19)*16/17.5=385$ M\$, or 28%. But this is unfair because the acceptances of the RLA were much larger than those in this pulsed synchrotron.

9 Parametric Studies

It is now interesting to ask what would be the costs for the same assumed acceptances. And interesting also, to see how these costs vary with the requirement for decay loss. To do this, we can attempt to write the costs as a simple formula based on the above costing.

We can then follow the same design procedures followed for this case, for other cases, and look at the resulting costs. It is important to understand that this is even less exact than the costing done for the above baseline. As the parameters vary greatly from the baseline, it is by no means certain that the resulting design is realistic. Nevertheless, the exercise is worth recording.

9.1 Pulsed Synchrotron Costing Formula

For Pulsed Synchrotron we will use

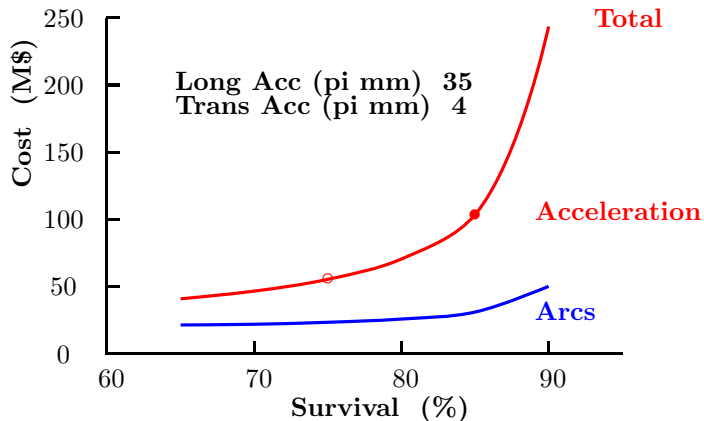
$$\text{Cost} = .048 V + 9.8 U + 4 U \sqrt{f \text{ (kHz)}} + 18.9 L(\text{m})$$

where the cost is in \$s, V is in Volts, and the L's are in m.

The pulsed power supply costs used here reflect a lower cost estimate for the chokes, and includes an optimization not included in the baseline, but the conclusions of the study do not depend on these details. Indeed the differences are well within the errors.

In each case, the same procedure was followed as outlined in section 5. i.e. We re-calculate the required apertures for the acceptance under consideration, and vary the combined function gradient and minimize the magnet + RF cost.

9.2 Cost vs. Allowed Decay Loss



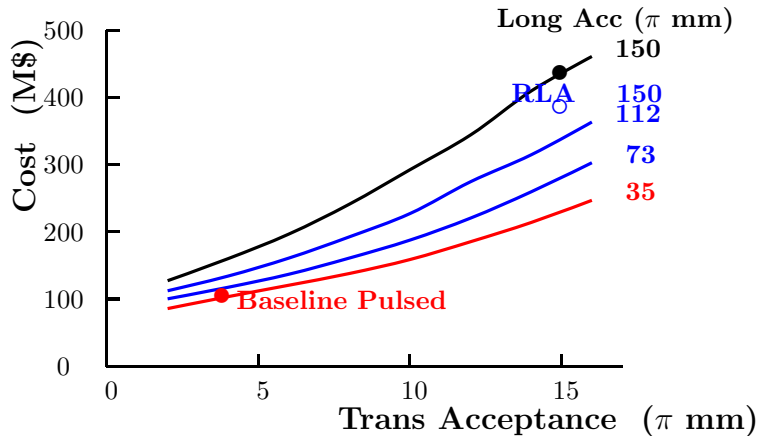
The above figure shows the pulsed synchrotron cost plotted versus the specified decay loss, with the acceptances used in the baseline. The total cost was divided, with suitable partition of civil costs, into those associated with the arcs (dominated by the pulsed magnets and power supplies) and those associated with the acceleration straight sections (dominated by the SC cavities and RF supplies). The blue line shows the arc contribution. The space between the blue line and the red total, indicates the RF contribution.

As greater decay loss is allowed, the RF per turn drops and this contribution to the cost falls. The drop in the arc cost, though smaller than that for the RF, arises because of the optimization of the bending magnet gradient. For low loss, and large RF costs, the optimization favors a stronger bending, to keep the circumference down, but this implies larger apertures and thus increased arc cost. As more loss is allowed, more turns are used, there is less RF cost,

but also less magnet cost because the optimization now favors smaller aperture magnets at the cost of less bending.

It is seen that there is a factor of 2 saving if the loss is allowed to grow from 15% to 25% (transmission falling from 75% to 85%). Such a large saving for only a 10% performance loss can probably be made up more cheaply in other ways, and is thus probably a reasonable compromise.

9.3 Cost vs. Acceptance



In this figure we plot the costs as a function of transverse acceptance for 4 different longitudinal acceptances. For comparison, the Study 2 RLA cost is also shown as a circle.

The above plot shows that for Study-2 acceptance, the pulsed synchrotron cost is \approx that of the RLA. This raises a number of questions:

- would an RLA with the lower acceptances used for the baseline also cost the same?
- How do these costs vary with decay loss.
- What are the costs for the intermediate case produced with one cooling ring: with the same transverse acceptance as study 2, but a smaller longitudinal acceptance.

9.4 Comparison of Pulsed Synchrotron vs. RLA Costs

To obtain an estimate of RLA costs under the different acceptance specifications, we will assume the same magnet optimization as is done for the pulsed machine. But now the arc costs are multiplied by number of turns that give a specified decay loss.

We can use the same SC RF, vacuum, diagnostic and conventional facility costs as in the pulsed magnet study, but we need a different cost estimate for the

conventional dipole and quadrupole magnets. For simplicity, we have assumed costs linear in the arc magnet stored energy, with a fixed 20% added to cover linac quadrupoles. The proportionality has been set such as to reproduce the Study 2 RLA total cost, and turns out to be 2.0 \$/J for the arc magnets, which is close to 1.93 \$/J Fermi Booster costs quoted above (Section 8.2).

The resulting RLA cost formula is:

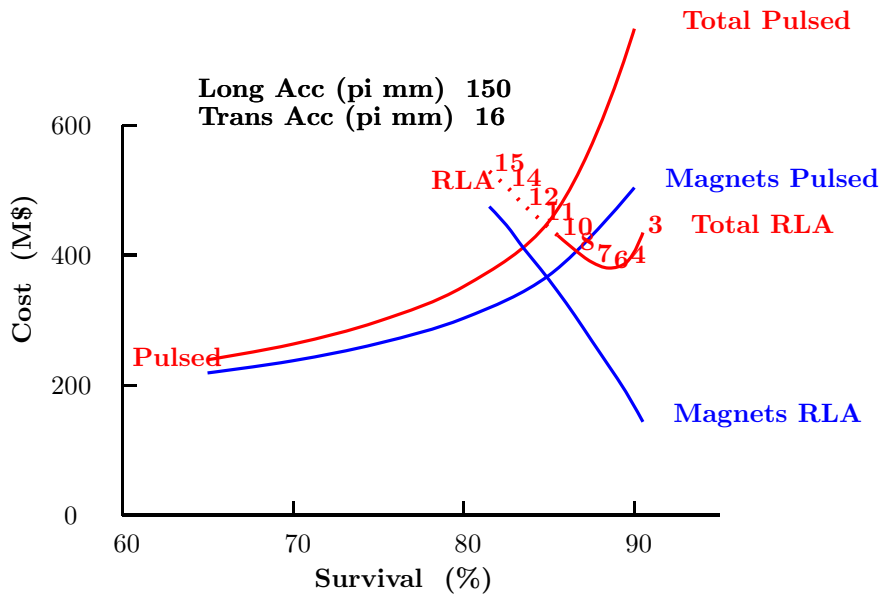
$$\text{Cost} = .048 V + 2.4 U n_{\text{turns}} + 13 (L_{\text{str}} + L_{\text{arc}}) + 5.8 (L_{\text{str}} + L_{\text{arc}} n_{\text{turns}})$$

where the cost is in \$s, V is in Volts, and the L's are in m.

In the following plots, we give costs for both pulsed and RLA's plotted versus decay survival, for three acceptance requirements:

1. With study 2 assumptions
2. With acceptances corresponding to the use of a single cooling ring
3. With acceptances as for the baseline, assuming the use of 2 cooling rings.

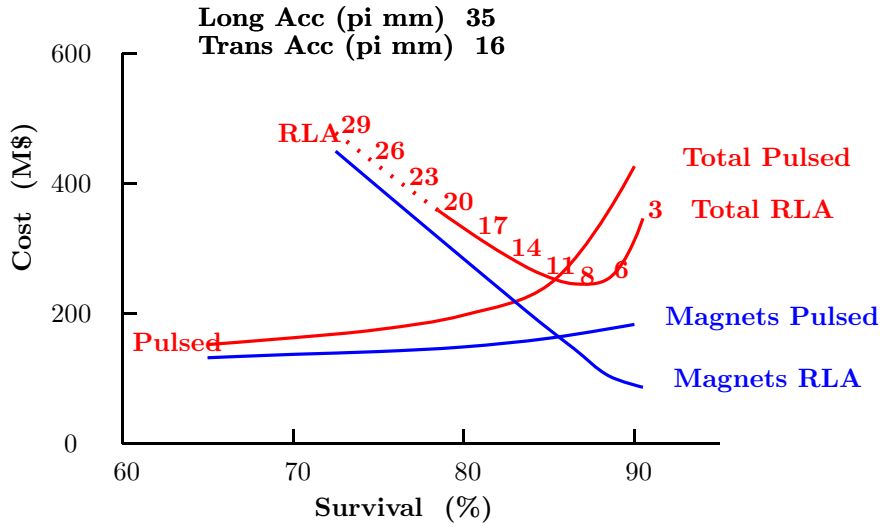
With Study-2 Acceptances



We note that:

- The pulsed synchrotron is cheaper if the allowed decay loss is greater than 18%
- and is 80% of the RLA for decay loss is 25%.

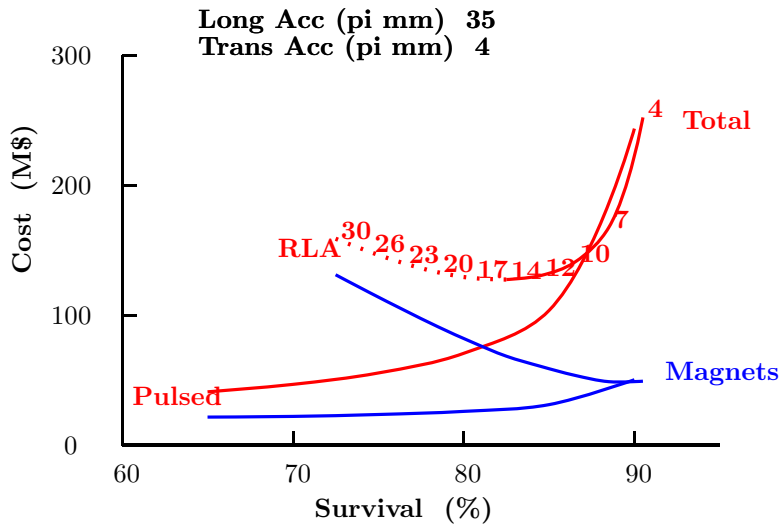
With Lower Long Acc (1 Cooling Ring)



We note that

- The pulsed design is cheaper for allowed decay loss is greater than 15 %.
- and is 71% of the RLA cost for allowed decay loss of 25 %.

With Lower Long. & Trans Acc (2 Cooling Rings)



We note that

- The pulsed design is cheaper than the RLA for allowed loss greater than 13%.
- and the pulsed design is 43% of RLA for allowed loss of 25%.

9.5 Summary of Pulsed vs. RLA comparisons

The general trend is that the savings if a pulsed synchrotron vs. an RLA increase as greater decay loss is accepted, and that this effect gets larger as the specified acceptances get smaller.

The numbers are summarized below.

	Study-2 Linear Cooling	1 Ring Cooling	2 Ring Cooling
Trans. Acceptance	15	15	4
Long. Acceptance	150	35	35
	π mm	π mm	π mm
	Costs		
	M\$	M\$	M\$
RLA	380	246	129 (229)†
Pulsed: 85 % Survival	450	245	104 (204)†
Pulsed: 75 % Survival	300	176	56 (156)†

We note that if we can accept 25 % decay loss, and use a single cooling ring instead of the linear channel of study-2, then the acceleration cost estimate is 176 M\$ compared with the RLA cost of 380 M\$: less than half.

The costs in parentheses and marked with †, have 100 M\$ added as a very rough approximation of that needed to pay for the second cooling ring required in these cases. With this very rough assumption, then with 2 cooling rings, the cost has come down an additional 20 M\$, which, though not significant, is in the right direction.

But in adding the 100 M\$ for the second ring, no additional correction was made for the likely savings in the Storage Ring with the resulting small required acceptances. This saving might be of the order 50 M\$ (out of 107 M\$), on the basis of the observed accelerator arc cost dependencies, and would give the same factor of two saving for this component.

10 Conclusion

- The cost of a combined function lattice, for a given acceptance, is minimized by the strongest possible field gradients, despite the resulting reduction in bending and resultant larger circumference.
- A DC, plus a bipolar pulsed current, appears cheaper than a simple monopolar magnet pulse.

- A preliminary cost estimate suggests that a low acceptance pulsed synchrotron might cost 27% of the Study 2 RLA. But since the acceptances are not the same, a scaling study was needed to estimate the real savings.
- This Scaling suggests:
 - For the same Study-2 acceptances and decay loss, the RLA and Pulsed costs are comparable in cost.
 - With acceptances from one Cooling Ring, and 25% decay, the cost of a pulsed synchrotron is estimated to be 71% of that for an RLA with the same acceptance, and 46% of that for the study-2 RLA.
 - With possible required acceptances after 2 Cooling Rings, the costs of both systems are further reduced, but with the second ring included, total costs appear similar to those with one Ring.
 - But the use of the second cooling ring would be expected to also reduce the cost of the storage ring, perhaps by a factor as large as 1/2. And would offer many other advantages.
- More study is needed to see if these saving survive engineering, and to see if the required performance can be achieved using the cooling rings assumed.